

International Journal of Polymer Analysis and Characterization

ISSN: 1023-666X (Print) 1563-5341 (Online) Journal homepage: www.tandfonline.com/journals/gpac20

Synthesis and characterization of unsaturated bio-based poly(propylene malonate- propylene fumarate)

Ersan Eyiler, Sevgi Sarigul-Ozbek & Ebru Erünal

To cite this article: Ersan Eyiler, Sevgi Sarigul-Ozbek & Ebru Erünal (19 Nov 2026): Synthesis and characterization of unsaturated bio-based poly(propylene malonate-propylene fumarate), International Journal of Polymer Analysis and Characterization, DOI: 10.1080/1023666X.2026.2716691

To link to this article: https://doi.org/10.1080/1023666X.2026.2716691

Published online: 19 Nov 2026.

Submit your article to this journal

View related articles

View Crossmark data

Full Terms & Conditions of access and use can be found at
https://www.tandfonline.com/action/journalInformation?journalCode=gpac20

INTERNATIONAL JOURNAL OF POLYMER ANALYSIS AND CHARACTERIZATION
https://doi.org/10.1080/1023666X.2026.2716691

Taylor & Francis
by informa

Check for updates

Synthesis and characterization of unsaturated bio-based poly(propylene malonate- propylene fumarate)

Ersan Eyiler[a], Sevgi Sarigul-Ozbek[b] and Ebru Erünal[c]

[a]Department of Chemical Engineering, Cukurova University, Adana, Turkey; [b]Faculty of Pharmacy, Department of Analytical Chemistry, Acıbadem Mehmet Ali Aydınlar University, İstanbul, Turkey; [c]Faculty of Engineering, Department of Chemical Engineering, Gebze Technical University, Kocaeli, Turkey

ABSTRACT

Bio-based monomers produced from biomass are attractive building blocks for the preparation of unsaturated polyesters with tunable properties. In this study, fully bio-based unsaturated copolyesters were synthesized by the incorporation of malonic acid (MA) into a combination of 1,3-propanediol (PDO) and fumaric acid (FA). The copolyesters with varying acid ratios were prepared using titanium (IV) butoxide as a transesterification catalyst through a melt polycondensation reaction. Their chemical and thermal properties were examined in detail by FT-IR spectroscopy, TGA, DSC,[1] H, and ^{13}C NMR spectroscopies. The results demonstrated that the thermal and crystallization behavior of the copolyesters could be effectively tailored by adjusting the monomer composition. Increasing the FA content promoted crystallization, resulting in semicrystalline copolyesters with melting temperatures of up to 118 °C, whereas MA-rich compositions remained predominantly amorphous with lower glass-transition temperatures. The copolyesters also exhibited good thermal stability, with maximum degradation temperatures ranging from 347 to 400 °C. Besides, it was verified that especially when the monomer ratios were close, the products had a more ordered structure. Overall, the results demonstrate that varying the MA/FA ratio provides an effective strategy for tailoring the thermal behavior and crystallinity of fully bio-based unsaturated copolyesters while maintaining good thermal stability.

ARTICLE HISTORY
Received 7 November 2025
Accepted 4 August 2026

KEYWORDS
Bio-based polyesters; polycondensation; biomass

Introduction

Unsaturated polyesters (UPs) have recently received great attention since the unsaturated bonds allow post- functionalization/polymerization that offers excellent thermal and mechanical properties.[1] This superior property makes them suitable for a wide range of applications, including aerospace, automotive, biomedical devices, and construction.[2] However, most commercial UPs have been produced from fossil resources, which increases global concerns in terms of environmental sustainability. Therefore, it is crucial to develop novel bio-based materials. In this manner, appropriate bio-based monomers produced from biomass are the ideal materials to prepare UPs with promising properties for certain applications.[3,4]

As a promising way to develop tailor-made aliphatic homo/copolyesters with excellent properties, different bio-based monomers were used and explored. For example, bio-based aliphatic polyesters based on sebacic acid, itaconic acid, 1,4-butanediol, 1,3-propanediol, succinic acid, 2,5-furandicarboxylic acid, adipic acid, glycerol, and others have been frequently studied in the

CONTACT Ebru Erünal ebruerunal@gtu.edu.tr Faculty of Engineering, Department of Chemical Engineering, Gebze Technical University, Kocaeli, Turkey
© 2026 Taylor & Francis Group, LLC

last 20 years, covering from rigid plastics to soft elastomers.[5–9] Among them, 1,3-propanediol (PDO) is one of the promising biomonomers that can be extracted via fermentation from many plants, such as corn. Poly(1,3-propylene terephthalate), commercially available (Sorona, Dupont), is one of the intensively studied 1,3-PDO-based polyesters.[10] Fumaric acid (FA) is one of the 12 building block chemicals identified by the U.S. Department of Energy in 2004 derived from sugars that can serve as key feedstocks for future biorefineries due to their functionality, availability, toxicity, and possible derivatives.[11] Also, the synthesis of FA-based polymers by polycondensation can be performed easily due to the high energy stability of C = C in FA.[12] Another bio-based monomer, malonic acid (MA), is a dicarboxylic acid produced from glycerol and can be used as a monomer or a crosslinker.[13,14] In addition, esterification was obtained by using dicarboxylic acids including MA as the crosslinking agent to crosslink polyvinyl alcohol (PVA).[15] Dogan and Kusefoglu[13] examined the polymerization of MA with soybean oil with some degree of success. Thus, the polymerization of MA presents an excellent opportunity for future studies in this area.

Recently, various biodegradable aliphatic polyesters based on these three monomers, such as poly(1,3-propylene malonate),[16] poly(1,3-propylene fumarate) (PPF),[17] and poly(ethylene glycol fumarate),[18] have been studied to investigate the superior properties of both corresponding monomers. These polymers often exhibit a unique combination of characteristics, including improved processability and tunable degradation rates, making them highly desirable for diverse applications. Synthesis of PPF via step polymerization for biomedical applications and the relation between the degradation kinetics and mechanical strength as a function of molecular weight and cross-linking agents have been widely studied in literature.[19–21] Synthesis of biobased block copolyesters via melt polycondensation from renewable monomers, such as glycerol, levulinic acid, malonic acid, and itaconic acid showed the potential of tuning the polymer properties throughout the variation of the initial monomer ratios.[22] Besides, in a previous study, novel bio-based polyesters, poly(propylene malonate) (PPM), and poly(propylene itaconate) (PPI), were synthesized by following green chemistry principals, and these polyesters belong to the polyhydroxyalkanoates (PHAs) family.[23] In this study, the incorporation of malonic acid into a combination of 1,3-propanediol and fumaric acid was investigated through the melt polycondensation method with the help of titanium(IV) butoxide as a transesterification catalyst. Chemical structures of the products were determined by NMR, and together with FTIR and thermal properties of the polyesters, they were examined by TGA/DSC to understand crystallinity and related properties as a function of changing dicarboxylic acid ratios.

Materials and methods

Materials

1,3-Propanediol (PDO, 98%), malonic acid (MA, 99%), fumaric acid (FA, 99%), titanium (IV) butoxide (TBT, $Ti(OBu)_4$, 97%), 4-methoxyphenol (99%), and all solvents were purchased from Sigma-Aldrich. All reagents and solvents were used as received without further purification.

Synthesis of copolyesters

Copolyesters with various dicarboxylic acid molar ratios were produced by a melt polycondensation method. The molar ratio of alcohol:acid monomer was kept constant at 1.2:1 in all trials while the molar ratios within the acids (MA/FA) were changed by the ratios of 100/0, 80/20, 60/40, 50/50, 40/60, 20/80, 0/100. At the esterification step, only low molecular weight oligomers formed. Then, at the polycondensation, the temperature was increased while the reaction pressure was decreased to provide the coupling of the oligomer chains by either an esterification or a transesterification reaction. The experiments were run in a 100 mL round-bottom flask equipped with a distillation setup and a nitrogen inlet to remove water and other by-products. The

reaction mixture with 4-methoxyphenol as a radical inhibitor (0.5 wt % to all reactants) was continuously stirred at 250 rpm and 135 °C for 3 h under a nitrogen atmosphere to limit oxidation. After oligomerization, at the polycondensation step, transesterification catalyst titanium (IV) butoxide ($Ti(OBu)_4$) was introduced at the melting of the mixture. Then, the reaction mixture was subsequently heated to 180 °C. A vacuum of 7 mbar was applied for another 3 h to remove water vapor. Following the polymerization, the reaction products were dissolved in chloroform and then precipitated in cold methanol (–30 °C) to remove the unreacted monomers and catalyst. Precipitated polymers were then filtered and dried in a vacuum oven at room temperature for 24 h. The poly(propylene malonate-propylene fumarate) (PPMF) copolyesters synthesized with different MA/FA molar ratios (100/0, 80/20, 60/40, 50/50, 40/60, 20/80, and 0/100) were named as "PP-M_xF_y" where x and y are the molar proportion of malonate and fumarate. The two homopolyesters (PP-$M_{100}F_0$ and PP-M_0F_{100}) were named PP-M and PP-F, respectively.

Characterization

The synthesized copolyesters were characterized by Fourier transform infrared spectroscopy (FTIR) using an ATR crystal Thermo Scientific instrument at a 600–4000 cm^{-1} wavelength range with a resolution of 4 cm^{-1} and 64 scans per run. Differential scanning calorimetry (DSC) was performed using a Mettler Toledo instrument under N_2 atmosphere with a flow rate of 40 mL/min. The samples were heated from room temperature to 160 °C at a rate of 10 °C/min and held for 3 min to eliminate the thermal history. Then, they were cooled to –60 °C and heated again from –60 to 160 °C at a rate of 10 °C/min. Thermogravimetric analysis (TGA) was performed using a Mettler Toledo instrument from room temperature to 600 °C at a heating rate of 10 °C/min under a nitrogen atmosphere. ^1H NMR and ^{13}C NMR spectra were collected by a Bruker Avance 300 MHz NMR instrument at room temperature using deuterated chloroform ($CDCl_3$) as the solvent.

Results and discussion

Chemical structure of copolyesters

The general copolymerization reaction of 1,3-propandiol (PDO), malonic acid (MA), and fumaric acid (FA) is given in Figure 1.

The formation of copolyesters for each sample was verified by FT-IR spectra, where the peaks obtained at 1753, 1722, and 1695 cm^{-1} correspond to ester bonds, as shown in Figure 2. As the ratio of fumaric acid increases, the peaks at 1753 and 1722 cm^{-1} increase while the peak at 1695 cm^{-1} decreases.

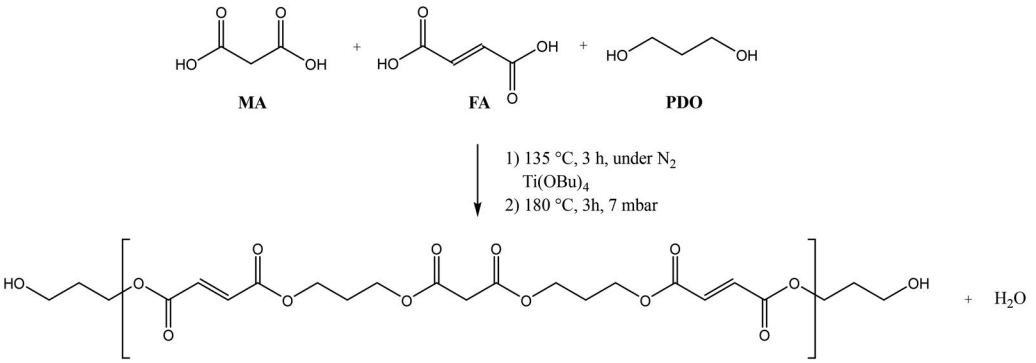


Figure 1. Copolymerization reaction of 1,3-propandiol (PDO), malonic acid (MA), and fumaric acid (FA).

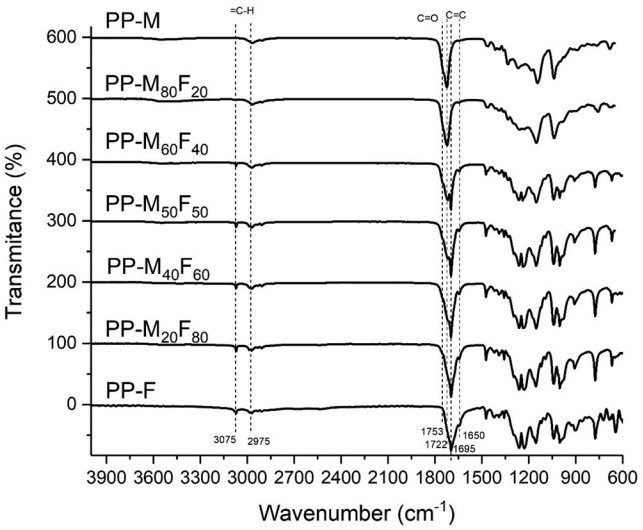


Figure 2. FT-IR spectra of the samples with varying ratios of malonic acid/fumaric acid.



Figure 3. The synthesized copolyesters according to varying malonic acid (MA)/fumaric acid (FA) ratios; from left to right PP-M, PP-$M_{80}F_{20}$, PP-$M_{60}F_{40}$, PP-$M_{50}F_{50}$, PP-$M_{40}F_{60}$, PP-$M_{20}F_{80}$.

In FT-IR measurements, when MA is used as the only acid monomer (PP-M), mostly -C = O stretching of esters at around 1700 cm^{-1} is tracked for PP-M since the reaction between the acid and alcohol yields an ester. When two acids (MA and FA) are present together in the reaction media, =C-H and -C = O stretchings are better seen. On the other hand, for PP-F, an additional -C = C- stretching around 1650 cm^{-1}[24] is expected since FA contains a double bond in the structure. Therefore, when only-MA (PP-M) or only-FA (PP-F) was present in the reaction media, only one sharp peak was observed at 1722 cm^{-1} for the former and at 1695 cm^{-1} for the latter, confirming the formation of the ester bonds. The small shift in the signal was seen because of the presence of an α,β-unsaturated system for the latter case. When the amount of FA increased, small peaks at 3075 and 1650 cm^{-1} belonging to = C-H and -C = C- stretching, respectively, started to be seen. By changing the MA/FA ratio, detection of two signals at around 1650–1750 cm^{-1} pointed to the formation of two types of ester bonds in the polymer chains due to the presence of two types of acid monomers. In addition, no peak corresponding to the -COOH peak was observed,[24] meaning that the end group of the products is not an acid group.

The synthesized copolyesters were shown in Figure 3. PP-M has a white color and soft structure. Especially the PP-$M_{80}F_{20}$ sample visually resembles polybutadiene with a semi-permeable yellowish color and elastic nature. However, when the fumaric acid ratio increased, the elastic image disappeared, and more rigid particles were obtained with higher fumaric acid amounts. The color also turned into opaque white and beige.

The solubility of samples was quite low in tetrahydrofuran (THF) and other solvents, which may be attributed to increased molecular weight, crystallinity, and/or strong chain packing.[25] Only the samples PP-$M_{40}F_{60}$, PP-$M_{50}F_{50,}$ and PP-$M_{60}F_{40}$ were soluble in chloroform. Hence, the ^{1}H NMR and ^{13}C NMR spectra of these three copolymers were taken in $CDCl_3$ and given in Figures 4 and 5. In the ^{1}H NMR spectra of the products (Figure 4), no acid peak was observed in the corresponding region (11.0–13.0 ppm).[26,27] This result demonstrated that the ending group must be hydroxyl, as expected because of the use of an excess amount of alcohol (PDO) in the reaction. Since in all

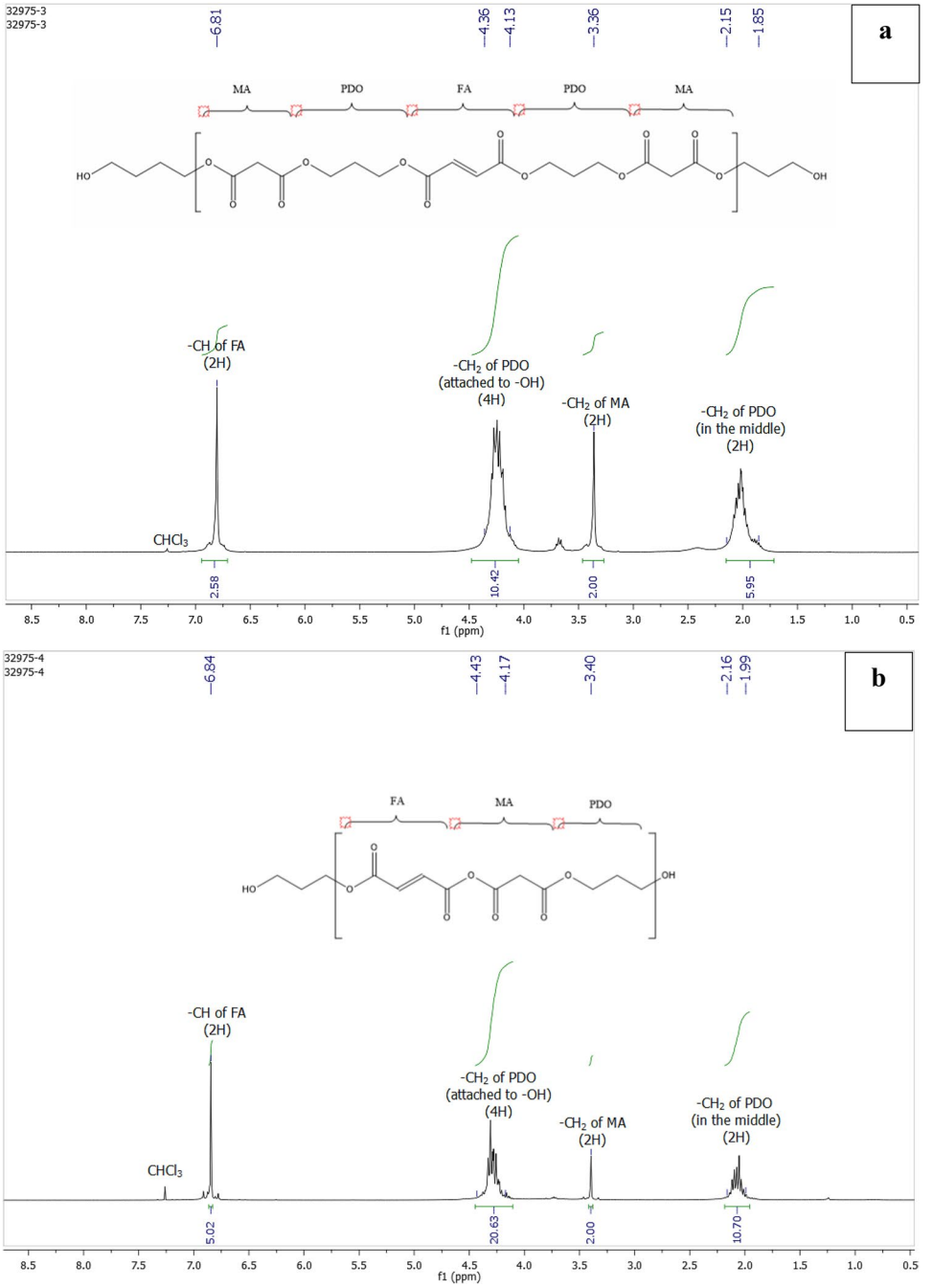


Figure 4.^{1}H NMR spectrum of the products (a) PP-$M_{60}F_{40,}$ (b) PP-$M_{50}F_{50,}$ and (c) PP-$M_{40}F_{60}$ taken in $CDCl_3$.

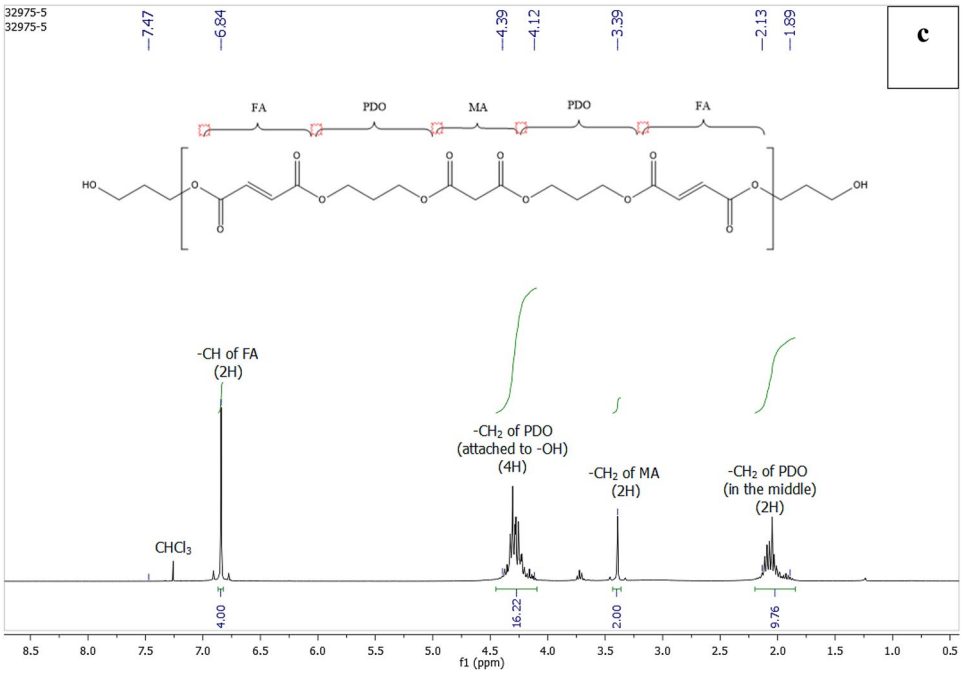
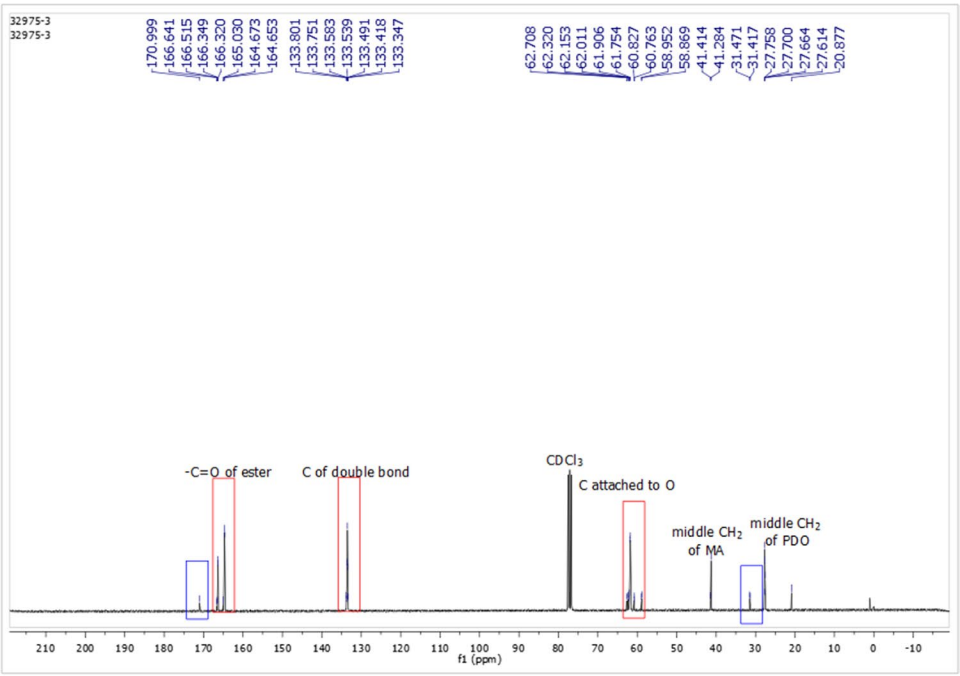


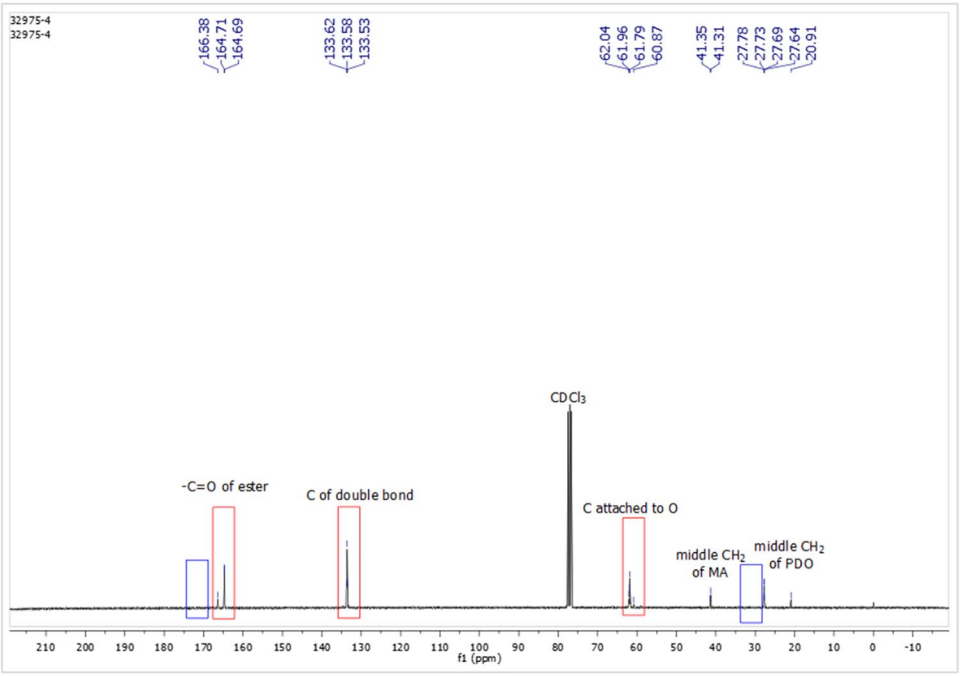
Figure 4. Cºntinued.

these products MA and FA were used together, the specific signals for each acid in the corresponding region should appear, which are a signal for two alpha hydrogens of MA at around 3.90–4.50 ppm[28] and that for the hydrogens attached to the double bond of FA at around 6.50–7.00 ppm,[29] respectively. In addition, multiplets at around 1.50–2.20 ppm for 2H and 4.00–4.50 ppm for 4H are also expected for the protons coming from PDO. The former is visible in a higher field since these hydrogens are further from the hydroxyl groups carrying an electronegative atom, while the latter appears in a lower field because these protons are direct neighbors of two OH groups. Furthermore, the integration between these multiplets should be 1:2 due to the number of hydrogens.

The ^{1}H NMR spectrum of PP-$M_{50}F_{50}$ (Figure 4(b)) gives the singlets at 3.40 ppm for 2H of MA and at 6.84 ppm for 2H of FA appeared, as expected. The integration ratio of these signals, belonging to the same number of hydrogens, was determined as 2.00:5.02 in favor of FA. This result demonstrates that the amount of FA units is more than that of MA in the product with a ratio of 2.51, although they are used in equal amounts, pointing to the higher reactivity of FA than MA in the transesterification reaction. In addition, the multiplets for the protons of PDO were observed in the corresponding regions (1.97–2.17 ppm and 4.13–4.43 ppm) with an integration ratio of 10.70:20.63, nearly as expected. The integration ratio of the same number of hydrogens (2H) of PDO to FA and MA was determined as 2.13 (10.70:5.02) and 5.35 (10.70:2.00). These ratios indicated that PDO has two- and five-times higher abundance in the structure compared to FA and MA, respectively. All these signals observed for the PP-$M_{50}F_{50}$ sample were also seen for the other copolymers (PP-$M_{60}F_{40}$ and PP-$M_{40}F_{60}$). Surprisingly, for PP-$M_{60}F_{40}$, the integration ratio between the protons of MA and FA was found to be 2.58:2.00, although FA was used in a lower percentage, 40%. For the same product, PDO/FA and PDO/MA ratios were determined as 2.31 (5.95:2.58) and 2.98 (5.95:2.00) based on the integration ratios obtained in ^{1}H NMR (Table 1). These ratios demonstrate that PDO is present nearly two times higher than FA and three times higher than MA in addition to having a higher number of FA units than the number of MA units. The copolymer compositions estimated from the integrations indicate that FA units are incorporated preferentially relative to the feed composition. This trend suggests that FA exhibits higher reactivity than MA under applied reaction conditions. Table 1 summarizes the chemical shifts of the signals seen in ^{1}H NMR together with the



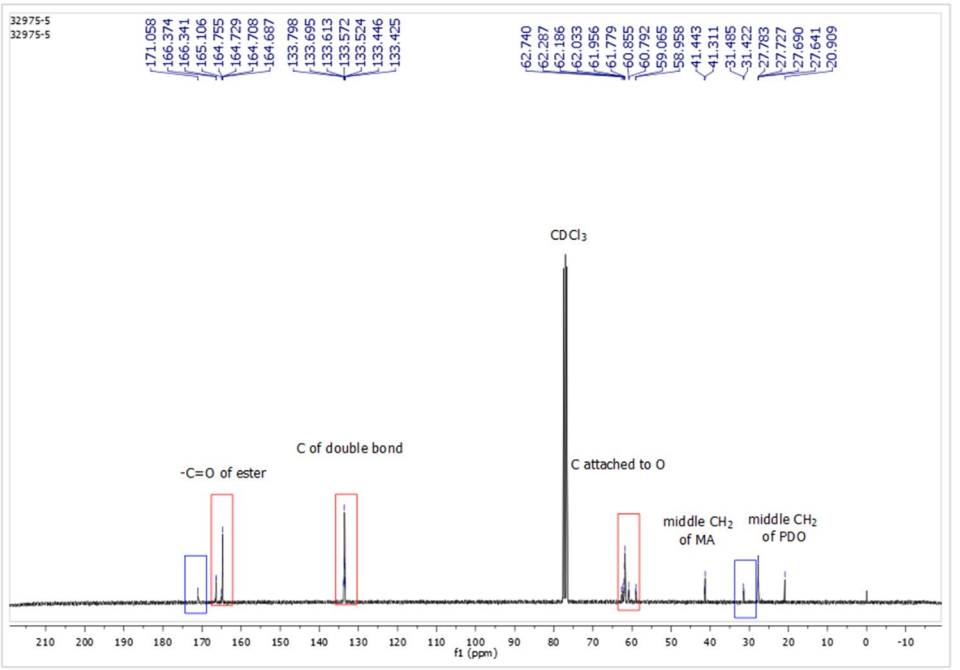
(a)



(b)

Figure 5.[13]C NMR spectrum of the products (a) PP-$M_{60}F_{40,}$ (b) PP-$M_{50}F_{50,}$ and (c) PP-$M_{40}F_{60}$ taken in $CDCl_3$.

integration ratios and molecular weights. The number-average molecular weights (Mn) of the copolyesters were determined by ^{1}H NMR end-group analysis using the ratio of the backbone 1,3-propanediol methylene protons (δ 4.25 ppm) to the terminal hydroxyl methylene protons (δ 3.70 ppm). The calculated Mn values ranged from 1.7 to 2.1 kg mol^{-1}. A gradual decrease in Mn was observed with increasing fumarate content, from 2.1 kg mol^{-1} for PP-$M_{60}F_{40}$ to 1.7 kg



(c)

Figure 5. C[on]tinued.

Table 1. The molecular weights, chemical shifts, and the integration ratios of the signals seen in ^{1}H NMR.

Product	Feed ratio MA/FA (mol%)	^{1}H NMR ratio MA/FA (mol%)	^{1}H NMR Mn (kg/mol)	-CH_2 of FA ppm	-CH_2 of FA int.	-CH_2 of PDO* ppm	-CH_2 of PDO* int.	-CH_2 of MA ppm	-CH_2 of MA int.	-CH_2 of PDO** ppm	-CH_2 of PDO** int.
PP-$M_{60}F_{40}$	60/40	43.7/56.3	2.1	6.81	2.58	4.36–4.13	10.42	3.36	2.00	2.15–1.85	5.95
PP-$M_{50}F_{50}$	50/50	28.5/71.5	1.9	6.84	5.02	4.43–4.17	20.63	3.40	2.00	2.16–1.99	10.70
PP-$M_{40}F_{60}$	40/60	33.3/66.7	1.7	6.84	4.00	4.39–4.12	16.22	3.39	2.00	2.13–1.89	9.76

*-CH_2 of PDO are the hydrogens attached to -OH's.
**-CH_2 of PDO are the hydrogens in the middle).

mol^{-1} for PP-$M_{40}F_{60}$. This trend suggests that higher fumaric acid incorporation limits chain growth during polycondensation, likely because of the increased rigidity associated with the unsaturated fumarate units, resulting in shorter polymer chains.

In ^{13}C NMR (Figure 5), the signals corresponding to the carbonyl carbon of the esters (165–170 ppm), the C's of the double bond due to the presence of the FA unit (130–135 ppm), the alpha carbons of the MA unit (40–45 ppm), the C's attached to the hydroxyl (60–65 ppm), and that in the middle of the PDO (25–30 ppm) were all observed in the expected chemical shift ranges. All these signals are summarized in Table 2. The spectrum belonging to the product obtained for PP-$M_{60}F_{40}$ and PP-$M_{40}F_{60}$ gave the same spectrum in terms of not only the chemical shifts but also the number of carbon signals. Both showed eight, seven, and five different carbon signals for each corresponding unit, except for α-C's of MA and the middle carbon between two OH of PDO, which produced two different signals in all three spectra. However, the ^{13}C NMR spectrum of the copolymer PP-$M_{50}F_{50}$ yielded a smaller number of signals in the corresponding region (Figure 5(b)). Since carbonyl carbons are affected by the chemical environment, the larger number of signals observed for the non-equimolar copolymers (PP-$M_{60}F_{40}$ and PP-$M_{40}F_{60}$) suggests the presence of a broader distribution of sequence arrangements and chemical environments along the polymer chain. In contrast, the reduced number of signals observed for PP-$M_{50}F_{50}$ indicates a

Table 2. Chemicals shifts of the products observed in ^{13}C NMR spectrum.

Product	-C=O of ester (ppm)	C of double bond (ppm)	C attached to oxygen (ppm)	CH_2 of MA (ppm)	CH_2 of PDO (ppm)
PP-$M_{60}F_{40}$	171.00, 166.64, 166.52, 166.35, 166.32 165.03, 164.67, 164.65 160.02, 157.81	133.80, 133.75, 133.58,133.54 133.49, 133.42, 133.35	62.71, 62.32, 62.15, 62.01, 61.91, 61.75, 60.83, 60.76, 58.95, 58.87	41.41, 41.28	31.47, 31.42 27.76, 27.70, 27.66, 27.61 20.88
PP-$M_{50}F_{50}$	166.38, 164.71, 164.69	133.62, 133.58, 133.53	62.04, 61.96, 61.79, 60.87,	41.35, 41.31	27.78, 27.73 27.69, 27.64 20.91
PP-$M_{40}F_{60}$	171.06, 166.37, 166.34 165.11, 164.75, 164.73, 164.71, 164.69	133.80, 133.70, 133.61, 133.57,133.52 133.45, 133.43	62.74, 62.29, 62.19, 62.03, 61.96, 61.78, 60.85, 60.79, 59.07, 58.96	41.44, 41.31	31.48, 31.42 27.78, 27.73 27.69, 27.64 20.91

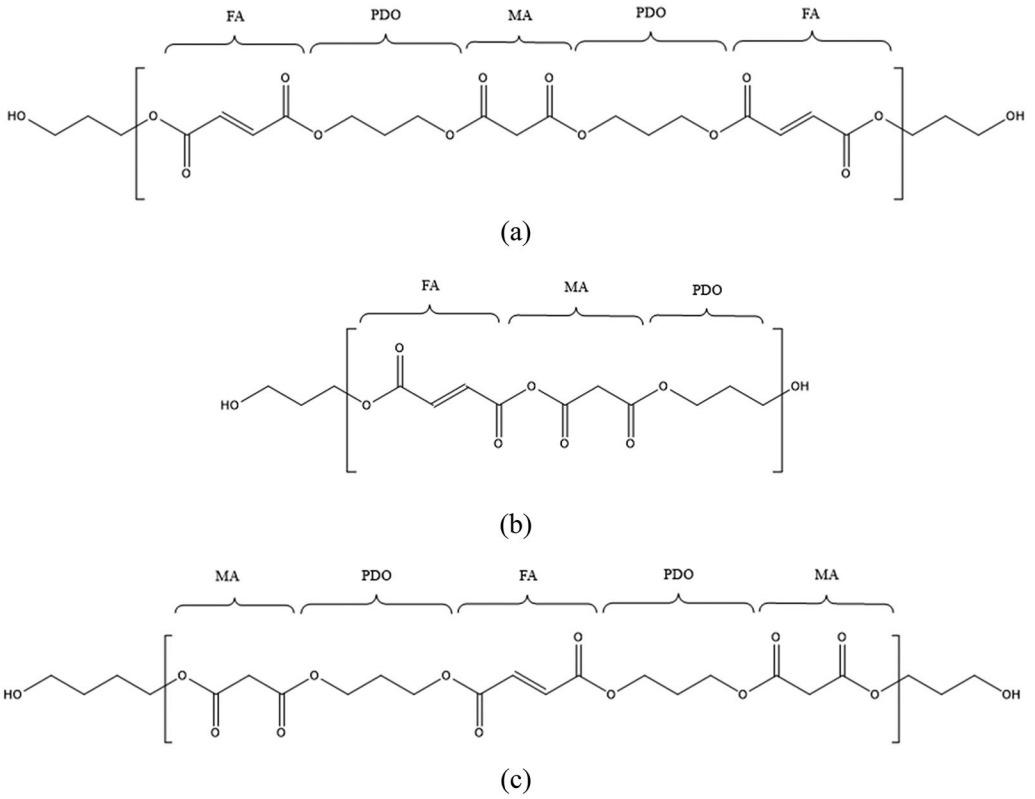


Figure 6. The proposed structures of the copolymers (a) PP-$M_{60}F_{40,}$ (b) PP-$M_{50}F_{50,}$ and (c) PP- $M_{40}F_{60}$ based on NMR observations.

more homogeneous structure with fewer distinct carbonyl environments. Therefore, we concluded that although the present data does not allow a definitive assignment of the chemical structure, the observations are consistent with a higher degree of structural regularity in the copolymer prepared from an equimolar MA&FA feed composition. The structures of the copolymers for PP-$M_{60}F_{40}$, PP-$M_{50}F_{50,}$ and PP-$M_{40}F_{60,}$ according to these findings, are proposed in Figure 6.

Table 3. Thermal properties of the obtained samples.

Sample	$T_{5\%}$ (°C)	$T_{10\%}$ (°C)	T_{max} (°C)	Residue at 600 °C (%)	T_g (°C)	T_m (°C)
PP-M	274	302	347	4	−43	
PP-$M_{80}F_{20}$	187	287	368	8	−11	
PP-$M_{60}F_{40}$	284	337	371	10	−31	
PP-$M_{50}F_{50}$	285	321	357	17	−28	94
PP-$M_{40}F_{60}$	279	312	380	18	−21	100
PP-$M_{20}F_{80}$	292	332	397	19	−15	118
PP-F	255	268	400	15	–	133

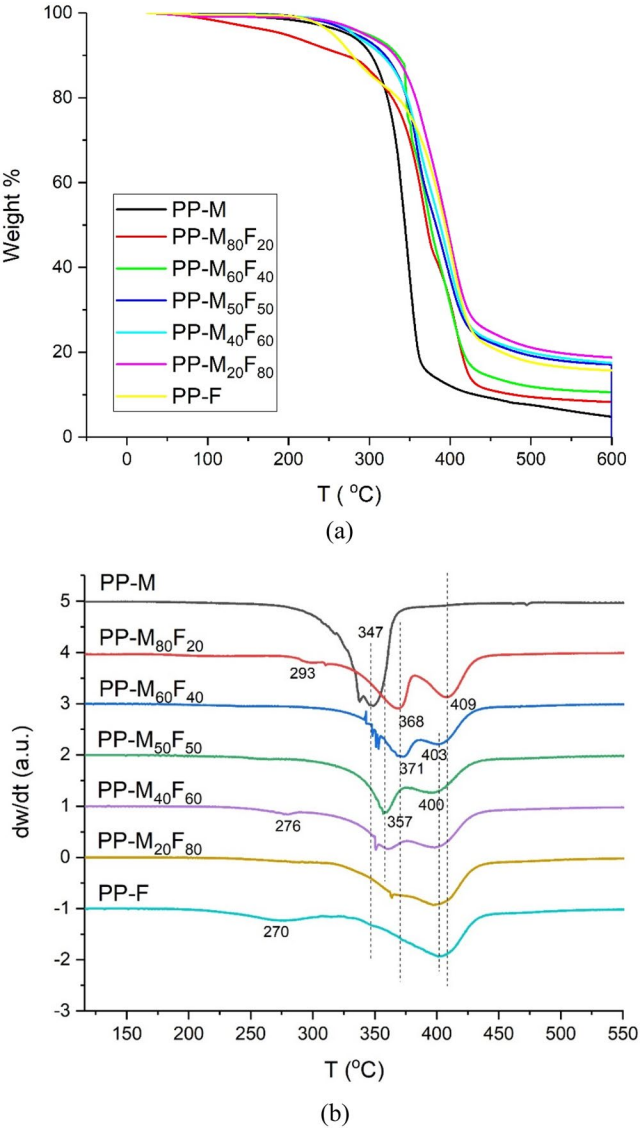


Figure 7. (a) Thermogravimetric analysis (TGA) and (b) derivative weight curves of the samples with varying dicarboxylic acid ratios.

Thermal properties

Thermal properties of the synthesized poly(propylene malonate-co-propylene fumarate) copolyesters were studied to understand their structure–property relationships and thermal behavior, and all data were summarized in Table 3. Figure 7 shows thermal gravimetric analysis (Figure 7(a)) and

the derivative of weight loss versus temperature (Figure 7(b)), while Figure 8 demonstrates differential scanning calorimetry measurements. $T_{5\%}$ refers to the temperature at 95% remaining mass, while $T_{10\%}$ refers to the temperature at 90% remaining mass. The intersection of the baseline with the tangent at the steepest decomposition region was shown as the residue at 600 °C as the T_{onset}. The copolyesters exhibited good thermal stability, with 5% weight-loss temperatures ($T_{5\%}$) ranging from 187 to 292 °C. Except for PP-$M_{80}F_{20}$, which showed the lowest $T_{5\%}$ (187 °C), the copolymers displayed initial degradation temperatures comparable to or higher than that of poly(propylene malonate) (PP-M, 274 °C). On the other hand, the only fumaric acid-containing material also seems highly thermally stable when compared to others in terms of the highest T_{max}. Moreover, intermediate compositions (especially 20–40% M) combine good onset stability with high T_{max}. Among the samples, PP-$M_{80}F_{20}$ has an unusual behavior with the lowest $T_{5\%}$ temperature and nearly 100 °C gap between $T_{5\%}$ and $T_{10\%}$. This suggests a small amount of material may decompose very early, but the bulk of the sample remains stable until much higher temperatures. This behavior can well be observed in the DTG shoulder around 293 °C, as seen in Figure 7(b). All in all, thermal gravimetric measurements and the derivative of weight loss with temperature are given to show that all bio-based materials have similar degradation temperatures to fossil-based plastics between 340 and 400 ^{0}C. Hence, the lowest degradation temperature was recorded for the material that has only malonic acid PP-M. As the malonic acid ratio decreases and the fumaric acid ratio increases, the degradation temperature of the samples raises nearly 50 °C. Similarly, the char residue at 600 °C increased from 4% for PP-M to 19% for PP-M20F80, suggesting improved thermal resistance and carbonaceous residue formation with increasing fumarate content.

The DSC analysis (Figure 8) indicated that samples containing higher amounts of malonic acid (MA) exhibit predominantly amorphous behavior, as evidenced by the presence of only glass transition temperature. The PP-M sample, which consists of only MA, showed a glass transition temperature (T_g) at −43 °C. By the addition of 20% fumaric acid (FA), it increased to −11 °C, suggesting reduced chain mobility. However, it should be noted that with the addition of more FA (PP-$M_{60}F_{40}$) during the esterification reaction, the end products possess a T_g around −31 °C. As the acid amounts become equal during esterification, a melting temperature is obtained around 94 °C. This indicates a semi-crystalline character for PP-$M_{50}F_{50}$ and suggests that balanced MA/FA incorporation promotes partial chain ordering. Since the melting temperature is an important parameter and preferred to be between 90 and 200 °C for the processing of plastics during extrusion, this material would be a good alternative for fossil-based plastics for various applications.[30] For compositions beyond the 50/50 ratio, all samples exhibited increased melting

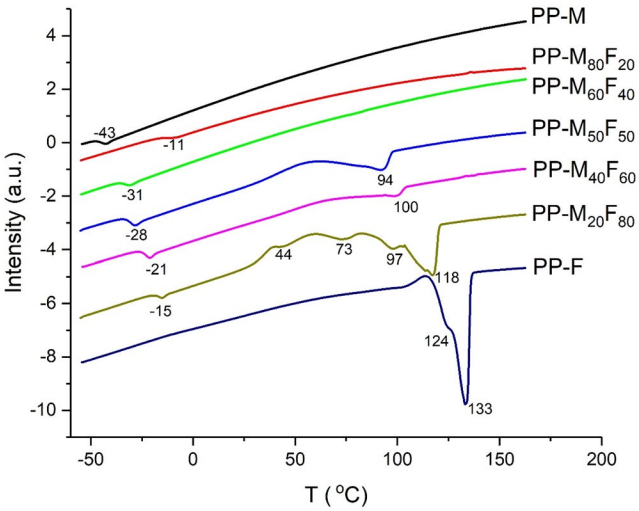


Figure 8. Differential Scanning Calorimetry (DSC) curves of the samples with varying dicarboxylic acid ratios.

transitions in DSC, indicating the development of crystalline domains depending on monomer composition. This thermal behavior toward a semi-crystalline character is also supported by NMR results where a more regular structure for PP-$M_{50}F_{50}$ was seen. This facilitates efficient chain packing, thereby suppressing the amorphous glass transition T_g while promoting the formation of a distinct crystalline phase with a melting temperature around 100 °C. However, shifting the feed toward one of the acid sources (either FA or MA) disrupts this structural regularity, leading to random amorphous segments with characteristic T_g.

Conclusions

The incorporation of malonic acid (MA) into a combination of 1,3-propanediol (PDO) and fumaric acid (FA) was investigated through a melt polycondensation method with the help of titanium(IV) butoxide as a transesterification catalyst. The formation of copolyesters was verified with FT-IR measurements, where the carbonyl stretching peaks around 1650–1750 cm^{-1} were determined regarding the formation of two different C = O stretches of the ester groups in the obtained products. The NMR measurements for chloroform-soluble samples (PP-$M_{60}F_{40}$, PP-$M_{50}F_{50}$ and PP-$M_{40}F_{60}$) suggested that copolymers synthesized at MA/FA ratios close to 50/50 exhibit a more regular and symmetric structure than those prepared at non-equimolar feed compositions. In addition, it can be concluded that under the applied reaction conditions FA is preferentially incorporated, suggesting higher reactivity of FA compared to MA. Hence, the variation of the acids did not affect the chemical structure of the copolymer unless they were used in equal amounts, which gives rise to a sequence of first acids and then alcohol. DSC measurements showed that samples containing more MA had amorphous structures with lower glass transition temperatures. However, copolymers containing 50 mol% or more fumarate, a semi-crystalline character, were obtained due to the melting temperature, indicating a more ordered structure which supports the observations in NMR, yet additional sequence-distribution analysis would be required. TGA showed that all bio-based materials had similar degradation temperatures to fossil-based plastics between 340 and 380 °C. Overall, the results demonstrate that varying the MA ratio provides an effective approach to tuning the thermal behavior and crystallinity of fully bio-based unsaturated copolyesters while maintaining their chemical structure and thermal stability.

Disclosure statement

No potential conflict of interest was reported by the author(s).

Data of data and materials

The manuscript has no associated data.

Author contributions

CRediT: **Ersan Eyiler**: Conceptualization, Data curation, Formal analysis, Investigation, Methodology, Validation, Writing – original draft, Writing – review & editing; **Sevgi Sarigul-Ozbek**: Data curation, Formal analysis, Investigation, Validation, Visualization, Writing – review & editing; **Ebru Erünal**: Conceptualization, Data curation, Formal analysis, Funding acquisition, Investigation, Methodology, Project administration, Resources, Supervision, Validation, Visualization, Writing – original draft, Writing – review & editing.

Funding

This project was funded by Çukurova University BAP Unit Project No FBA-2020-13171.

ORCID

Ersan Eyiler http://orcid.org/0000-0002-1754-6590
Sevgi Sarigul-Ozbek http://orcid.org/0000-0002-0676-2415
Ebru Erünal http://orcid.org/0000-0002-9926-2654

References

[1] Akbari, S., A. Root, M. Skrifvars, S. K. Ramamoorthy, and D. Åkesson. 2024. Novel bio-based branched unsaturated polyester resins for high-temperature applications. *J. Polym. Environ.* 32:2031–2044. doi:10.1007/s10924-023-02835-2
[2] Rizzo, G., S. Dattilo, V. Prasad, M. Yasar, A. Ivankovic, A. Latteri, and G. Cicala. 2024. Enhancing sustainability in unsaturated polyester resin: a way to use biobased curing agents for reduced styrene content and improved recyclability properties. *ACS Appl. Polym. Mater.* 6:5714–5725. doi:10.1021/acsapm.4c00441
[3] Bamane, P., K. Wadgaonkar, K. Srivastava, and R. Jagtap. 2022. The effect of partial replacement of maleic anhydride by itaconic acid in sebacic acid-based unsaturated polyester on its various properties. *J. Polym. Res.* 29:374. doi:10.1007/s10965-022-03284-5
[4] Llevot, A., P. K. Dannecker, M. von Czapiewski, L. C. Over, Z. Söyler, and M. A. Meier. 2016. Renewability is not enough: recent advances in the sustainable synthesis of biomass-derived monomers and polymers. *Chemistry* 22:11510–11521. doi:10.1002/chem.201601438
[5] Debuissy, T., E. Pollet, and L. Avérous. 2017. Synthesis and characterization of fully biobased poly(propylene succinate-ran-propylene adipate): analysis of the architecture-dependent physicochemical behavior. *J. Polym. Sci. Part A: Polym. Chem.* 55:2738–2748. doi:10.1002/pola.28656
[6] Guo, B., Y. Chen, Y. Lei, L. Zhang, W. Y. Zhou, A. B. M. Rabie, and J. Zhao. 2011. Biobased poly(propylene sebacate) as shape memory polymer with tunable switching temperature for potential biomedical applications. *Biomacromolecules* 12:1312–1321. doi:10.1021/bm101549t
[7] Papadopoulos, L., E. Xanthopoulou, G. N. Nikolaidis, A. Zamboulis, D. S. Achilias, G. Z. Papageorgiou, and D. N. Bikiaris. 2020. Towards high molecular weight furan-based polyesters: solid state polymerization study of bio-based poly(propylene furanoate) and poly(butylene furanoate). *Materials* 13:4880. doi:10.3390/ma13214880
[8] Tan, B., S. Bi, K. Emery, and M. J. Sobkowicz. 2017. Bio-based poly(butylene succinate-co-hexamethylene succinate) copolyesters with tunable thermal and mechanical properties. *Eur. Polym. J.* 86:162–172. doi:10.1016/j.eurpolymj.2016.11.036
[9] Robert, T., and S. Friebel. 2016. Itaconic acid – a versatile building block for renewable polyesters with enhanced functionality. *Green Chem.* 18:2922–2934. doi:10.1039/C6GC00605A
[10] Debuissy, T., P. Sangwan, E. Pollet, and L. Avérous. 2017. Study on the structure–properties relationship of biodegradable and biobased aliphatic copolyesters based on 1,3-propanediol, 1,4-butanediol, succinic and adipic acids. *Polymer.* 122:105–116. doi:10.1016/j.polymer.2017.06.037
[11] Werpy, T., G. Petersen, A. Aden, J. Bozell, J. Holladay, J. White, A. Manheim, D. Eliot, L. Lasure, and S. Jones. 2004. Top value added chemicals from biomass: results of screening for potential candidates from sugars and synthesis gas. *U.S. Department Energy Report.* 1:26–28.
[12] Yu, Y., H. Xiong, J. Xiao, X. Qian, X. Leng, Z. Wei, and Y. Li. 2019. High molecular weight unsaturated copolyesters derived from fully biobased trans-β-hydromuconic acid and fumaric acid with 1,4-butanediol: synthesis and thermomechanical properties. *ACS Sustain. Chem. Eng.* 7:6859–6869. doi:10.1021/acssuschemeng.9b00150
[13] Doğan, E., and S. Küsefoğlu. 2008. Synthesis and in situ foaming of biodegradable malonic acid ESO polymers. *J. Appl. Polym. Sci.* 110:1129–1135. doi:10.1002/app.28684
[14] Dastidar, T. G., and A. N. Netravali. 2012. 'Green' crosslinking of native starches with malonic acid and their properties. *Carbohydr. Polym.* 90:1620–1628. doi:10.1016/j.carbpol.2012.06.081
[15] Qiu, K., and A. N. Netravali. 2013. Halloysite nanotube reinforced biodegradable nanocomposites using non-crosslinked and malonic acid crosslinked polyvinyl alcohol. *Polym. Compos.* 34:799–809. doi:10.1002/pc.22445
[16] Campisano, I. S. P., E. de Queiros Eugenio, C. de Oliveira Veloso, M. L. Dias, A. M. de Castro, and M. A. P. Langone. 2021. Solvent-free lipase-catalyzed synthesis of linear and thermally stable polyesters obtained from diacids and diols. *Braz. J. Chem. Eng.* 38:549–562. doi:10.1007/s43153-021-00137-5
[17] Wei, X. W., X. X. Zhao, Y. Li, X. Y. Meng, Q. Zhou, and H. M. Ye. 2022. Distinctive polymorphism-like isodimorphism in poly(propylene succinate-ran-propylene fumarate). *Chin. J. Polym. Sci.* 40:602–610. doi:10.1007/s10118-022-2767-1
[18] Jo, S., H. Shin, A. K. Shung, J. P. Fisher, and A. G. Mikos. 2001. Synthesis and characterization of oligo(poly(ethylene glycol) fumarate) macromer. *Macromolecules.* 34:2839–2844. doi:10.1021/ma0018163
[19] Domb, A. J., C. T. Laurencin, O. Israeli, T. N. Gerhart, and R. Langer. 1990. The formation of propylene fumarate oligomers for use in bioerodible bone cement composites. *J. Polym. Sci. A. Polym. Chem.* 28:973–985. doi:10.1002/pola.1990.080280503

[20] Shung, A. K., M. D. Timmer, S. Jo, P. S. Engel, and A. G. Mikos. 2002. Kinetics of poly(propylene fumarate) synthesis by step polymerization of diethyl fumarate and propylene glycol using zinc chloride as a catalyst. *J. Biomater. Sci. Polym. Ed.* 13:95–108. doi:10.1163/156856202753525963
[21] Kasper, F. K., K. Tanahashi, J. P. Fisher, and A. G. Mikos. 2009. Synthesis of poly(propylenefumarate). *Nature* 4:518–525. doi:10.1038/nprot.2009.24
[22] Eyiler, E. 2025. Solvent-free one-pot sequential synthesis of biobased block copolyesters via melt polycondensation. *J. Macromol. Sci. Part A.* 62:1277–1285. doi:10.1080/10601325.2025.2581825
[23] Rowe, M. D., E. Eyiler, and K. B. Walters. 2016. Bio-based plasticizer and thermoset polyesters: a green polymer chemistry approach. *J. Appl. Polym. Sci.* 133:44145. doi:10.1002/app.44145
[24] He, Y., F. Ding, Y. Zhao, W. Tian, W. Feng, and H. Yan. 2022. Multicolor emission of nonaromatic linear polysiloxanes based on local conjugation chains. *Polym. Chem.* 13:6534–6542. doi:10.1039/D2PY00922C
[25] Yu, F., Y. Liu, X. Pan, X. Lin, C. Liu, P. Chen, and R. Ruan. 2006. Liquefaction of corn stover and preparation of polyester from the liquefied polyol. *Appl. Biochem. Biotechnol.* 130:574–585. doi:10.1385/abab:130:1:574
[26] Rashid, K. T., H. M. Alayan, A. E. Mahdi, M. N. Al-Baiati, H. S. Majdi, I. K. Salih, J. M. Ali, and Q. F. Alsalhy. 2022. Novel water-soluble poly(terephthalic-co-glycerol-g-fumaric acid) copolymer nanoparticles harnessed as pore formers for polyethersulfone membrane modification: permeability–selectivity tradeoff manipulation. *Water.* 14:1507. doi:10.3390/w14091507
[27] Durairaju, P., C. Umarani, J. R. Rajabather, A. M. Alanazi, G. Periyasami, and L. D. Wilson. 2021. Synthesis and characterization of pyridine-grafted copolymers of acrylic acid–styrene derivatives for antimicrobial and fluorescence applications. *Micromachines.* 12:672. doi:10.3390/mi12060672
[28] Byrne, F. P., J. M. Assemat, A. E. Stanford, T. J. Farmer, J. W. Comerford, and A. Pellis. 2021. Enzyme-catalyzed synthesis of malonate polyesters and their use as metal chelating materials. *Green Chem.* 23:5043–5048. doi:10.1039/D1GC01712G
[29] Ahmed, N. M., M. E. Tawfik, and A. A. Ward. 2013. Characterization of a polymer composite from treated kaolin and unsaturated polyester based on PET waste. *Polym. Compos.* 34:1223–1234. doi:10.1002/pc.22467
[30] Capone, C., L. Di Landro, F. Inzoli, M. Penco, and L. Sartore. 2007. Thermal and mechanical degradation during polymer extrusion processing. *Polym. Eng. Sci.* 47:1813–1819. doi:10.1002/pen.20891